

In Situ Immobilization of Metalloligands: A Synthetic Route to Homometallic Mixed-Valence Coordination Polymers

Wen-Xiu Ni, Mian Li, Shun-Ze Zhan, Jin-Zhang Hou, and Dan Li*

Department of Chemistry, Shantou University, Guangdong 515063, People's Republic of China

Received August 11, 2008

This work focuses on the investigation of targeting homometallic mixed-valence copper(I/II) Schiff base coordination polymers (CPs) via a proposed synthetic strategy, namely, in situ immobilization of metalloligands. We have designed and synthesized three structurally related isomeric Schiff base ligands, all of which contain chelating and bridging sites and, accordingly, obtained two distinctly shaped metalloligands, namely, $[\text{Cu}(\text{L1})_2]$ (**1**) and $[\text{Cu}(\text{L3})_2]$ (**3a**) [**HL** = pyridinecarbaldehyde isonicotinoyl hydrazone]. By introducing cyanide-bridging spacers to the one-pot solvothermal reactions, the copper(II) Schiff base metalloligands **1** and **3a** are in situ immobilized in two diverse mixed-valence copper(I/II) Schiff base CPs, namely, $[\text{Cu}_4(\text{CN})_3(\text{L1})_2]_n$ (**4**) and $\{[\text{Cu}_4(\text{CN})_3(\text{L3})_2] \cdot 2.5\text{H}_2\text{O}\}_n$ (**6**). Additionally, the formation of three unexpected CPs, namely, $[\text{Cu}(\text{L3})_2]_n$ (**3b**), $[\text{Cu}(\text{L2})_2]_n$ (**2**), and $[\text{Cu}_2(\text{CN})_2(\text{HL2})]_n$ (**5**), indicates that the coordinating sites of the ligands and the symmetry of the metalloligands should be taken into consideration in this synthetic algorithm.

Introduction

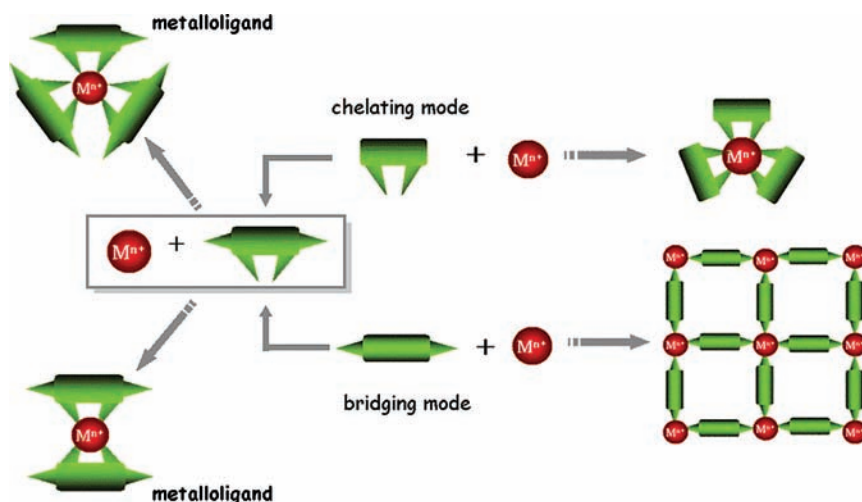
Inorganic chemists enjoy the luxury of the uncountable combination of metal ions and organic ligands for the construction of coordination polymers (CPs), and, therefore, the research in this field has undergone a tremendous burst over the past few decades.¹ From the viewpoint of crystal engineering, a general synthetic principle of “connectors and linkers” has been proposed^{1c} and is widely utilized for targeting various CPs via the judicious selection of metal centers and organic ligands.² In recent years, this principle has been specified and developed. Two alternative and complementary synthetic approaches emerge, that is, the

secondary building unit (SBU)³ and the metalloligand (ML).⁴ These two approaches are distinguishable, due to the following points: (i) An SBU involves two or more metal centers and is usually regarded as a “connector”, whereas an ML often contains one metal center and is treated as a “linker”. (ii) It is well-recognized that the immobilization of MLs into CPs requires stepwise synthesis, whereas the formation of SBUs can be achieved in one-pot synthesis. (iii) The SBU approach is useful for predesigning targeted

* To whom correspondence should be addressed. E-mail: dli@stu.edu.cn.

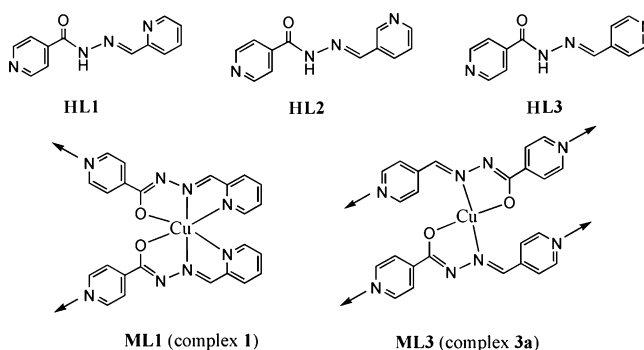
- (1) For reviews: (a) Batten, S. R.; Robson, R. *Angew. Chem., Int. Ed.* **1998**, *37*, 1460. (b) Moulton, B.; Zaworotko, M. J. *Chem. Rev.* **2001**, *101*, 1629. (c) Holliday, B. J.; Mirkin, C. A. *Angew. Chem., Int. Ed.* **2001**, *40*, 2022. (d) Yaghi, O. M.; O'Keefe, M.; Ockwig, N. W.; Chae, H. K.; Eddaoudi, M.; Kim, J. *Nature* **2003**, *423*, 705. (e) Kitagawa, S.; Kitaura, R.; Noro, S.-i. *Angew. Chem., Int. Ed.* **2004**, *43*, 2334. (f) Férey, G. *Chem. Soc. Rev.* **2008**, *37*, 191.
- (2) For examples: (a) Evans, O. R.; Lin, W. *Acc. Chem. Res.* **2002**, *35*, 511. (b) Rao, C. N. R.; Natarajan, S.; Vaidhyanathan, R. *Angew. Chem., Int. Ed.* **2004**, *43*, 1466. (c) Férey, G.; Mellot-Draznieks, C.; Serre, C.; Millange, F. *Acc. Chem. Res.* **2005**, *38*, 217. (d) Bradshaw, D. J.; Claridge, B.; Cussen, E. J.; Prior, T. J.; Rosseinsky, M. J. *Acc. Chem. Res.* **2005**, *38*, 273. (e) Feng, P.; Bu, X.; Zheng, N. *Acc. Chem. Res.* **2005**, *38*, 293. (f) Hill, R. J.; Long, D.; Champness, N. R.; Hubberstey, P.; Schröder, M. *Acc. Chem. Res.* **2005**, *38*, 335.

- (3) (a) Eddaoudi, M.; Moler, D. B.; Li, H.; Chen, B.; Reineke, T. M.; O'Keefe, M.; Yaghi, O. M. *Acc. Chem. Res.* **2001**, *34*, 319. (b) Kitagawa, S.; Furukawa, S. *Frontiers in Crystal Engineering*; John Wiley & Sons, Ltd.: New York, 2006; Chapter 9, p 195. (c) Kim, J.; Chen, B.; Reineke, T. M.; Li, H.; Eddaoudi, M.; Moler, D. B.; O'Keefe, M.; Yaghi, O. M. *J. Am. Chem. Soc.* **2001**, *123*, 8239. (d) Nouar, F.; Eubank, J. F.; Bousquet, T.; Wojtas, L.; Zaworotko, M. J.; Eddaoudi, M. *J. Am. Chem. Soc.* **2008**, *130*, 1833. (e) He, J.; Yin, Y.-G.; Wu, T.; Li, D.; Huang, X.-C. *Chem. Commun.* **2006**, 2845. (f) Li, Z.; Li, M.; Zhan, S.-Z.; Huang, X.-C.; Ng, S. W.; Li, D. *CrystEngComm* **2008**, *10*, 978.
- (4) (a) Abrahams, B. F.; Hoskins, B. F.; Michail, D. M.; Robson, R. *Nature* **1994**, *369*, 727. (b) Carlucci, L.; Ciani, G.; Porta, F.; Proserpio, D. M.; Santagostini, L. *Angew. Chem., Int. Ed.* **2002**, *41*, 1907. (c) Kitaura, R.; Onoyama, G.; Sakamoto, H.; Matsuda, R.; Noro, S.-i.; Kitagawa, S. *Angew. Chem., Int. Ed.* **2004**, *43*, 2684. (d) Murphy, D. L.; Malachowski, M. R.; Campana, C. F.; Cohen, S. M. *Chem. Commun.* **2005**, 5506. (e) Halper, S. R.; Do, L.; Stork, J. R.; Cohen, S. M. *J. Am. Chem. Soc.* **2006**, *128*, 15255. (f) Youm, K.-T.; Kim, M. G.; Ko, J.; Jun, M.-J. *Angew. Chem., Int. Ed.* **2006**, *45*, 4003. (g) Zhang, S.-S.; Zhan, S.-Z.; Li, M.; Peng, R.; Li, D. *Inorg. Chem.* **2007**, *46*, 4365.

Scheme 1. Illustration of the Difference between the Chelating or Bridging Mode of a Ligand

CPs and understanding their topological networks, and, in contrast, the ML strategy is a powerful tool for constructing heterometallic or homometallic mixed-valence CPs.^{1c}

Mixed-valence homometallic copper(I/II) complexes are important because the long-distance electron transfer observed in such entities would enable their application as electrochemical sensors or ferrimagnets, etc.⁵ However, the synthesis of this species encountered numerous obstacles, and, thus, only a few synthetic strategies on this topic have been documented to date.^{5a} The utilization of MLs is an attractive approach for targeting mixed-valence homometallic CPs, but the unreliable aspect of this strategy is that the stepwise synthetic procedure would inevitably reduce the reactivity and reaction yield. It is crucial that the chosen ML be soluble in water or common organic solvents to facilitate the second-step reaction, which deprives the opportunity for many poorly soluble precursor complexes to serve as potential MLs, especially for those obtained from hydro-(solvothermal) reactions. Our strategy to overcome this synthetic difficulty is to in situ immobilize copper(II) ML linkers into copper(I) connector-based CPs, by taking advantage of the distinct structure-defining roles of chelating and bridging ligands.⁶ As illustrated in Scheme 1, chelating ligands (e.g., 2,2'-bipyridine) were usually employed for the formation of discrete oligonuclear complexes, whereas bridging ligands (e.g., 4,4'-bipyridine) were normally used to construct extended CPs.⁷ A combination of both chelating and bridging modes in the multifunctional ligands is our rationale for targeting in situ immobilized MLs into CPs. In situ immobilization of MLs refers to a synthetic procedure

Chart 1. Series of Isomeric Schiff Base Ligands and Copper(II) Schiff Base Metalloligands (MLs)

that enables the MLs to be either isolated as discrete compounds or in situ formed (with the same archetypes of the discrete derivatives) and immobilized into CPs in the one-step syntheses (not the traditional stepwise syntheses for MLs).

In a recent communication, we reported that a Schiff base ligand (**HL3**) could be deprotonated under proper pH conditions, leading to the formation of a square-planar copper(II) Schiff base ML and, thus, increasing the structural dimensionality of the resulting CPs.⁸ We realized that this synthetic procedure might become a general route to homometallic mixed-valence copper(I/II) CPs. The chelating sites from two Schiff base ligands would stabilize the oxidation state of copper(II) via the formation of MLs, and other copper ions that serve as connectors would remain monovalent in solvothermal reactions.⁹ Accordingly, a series of previously reported Schiff base ligands, namely, 2- (**HL1**), 3- (**HL2**), and 4-pyridinecarbaldehyde isonicotinoyl hydrazone (**HL3**), are used in this work (see Chart 1, top row). All three ligands contain both appropriate chelating and bridging sites: the carbonyl O and imine N atoms will bind the metal ions in a chelating fashion, whereas the pyridyl N atoms show potential bridging character. We have obtained and charac-

(5) (a) Zhang, X.-M.; Tong, M.-L.; Chen, X.-M. *Angew. Chem., Int. Ed.* **2002**, *41*, 1029. (b) Zhang, X.-M.; Tong, M.-L.; Gong, M.-L.; Lee, H.-K.; Luo, L.; Li, K.-F.; Tong, Y.-X.; Chen, X.-M. *Chem.-Eur. J.* **2002**, *8*, 3187. (c) Zhang, X.-M.; Fang, R.-Q. *Inorg. Chem.* **2005**, *44*, 3955. (d) Zhang, X.-M.; Zhao, Y.-F.; Zhang, W.-X.; Chen, X.-M. *Adv. Mater.* **2007**, *19*, 2843. (e) Hou, L.; Li, D.; Shi, W.-J.; Yin, Y.-G.; Ng, S. W. *Inorg. Chem.* **2005**, *44*, 7825.
 (6) (a) Steel, P. J. *Acc. Chem. Res.* **2005**, *38*, 243. (b) Beauchamp, D. A.; Loeb, S. J. *Dalton Trans.* **2007**, 4760.
 (7) (a) Kaes, C.; Katz, A.; Hosseini, M. W. *Chem. Rev.* **2000**, *100*, 3553. (b) Serroni, S.; Campagna, S.; Puntoriero, F.; Pietro, C. D.; McClenaghan, N. D.; Loiseau, F. *Chem. Soc. Rev.* **2001**, *30*, 367. (c) Selby, H. D.; Roland, B. K.; Zheng, Z. *Acc. Chem. Res.* **2003**, *36*, 933.

(8) Ni, W.-X.; Li, M.; Zhou, X.-P.; Li, Z.; Huang, X.-C.; Li, D. *Chem. Commun.* **2007**, 3479.

(9) (a) Zhang, X.-M. *Coord. Chem. Rev.* **2005**, *249*, 1201. (b) Chen, X.-M.; Tong, M.-L. *Acc. Chem. Res.* **2007**, *40*, 162.

terized two structurally isomeric copper(II) Schiff base MLs, namely, $[\text{Cu}(\text{L1})_2]$ (**1**) and $[\text{Cu}(\text{L3})_2]$ (**3a**) (see Chart 1, bottom row), as well as two related polymeric compounds, $[\text{Cu}(\text{L2})_2]_n$ (**2**) and $[\text{Cu}(\text{L3})_2]_n$ (**3b**) (**3a** and **3b** are concomitant genuine isomers). Though complexes **1–3** are all poorly soluble in common organic solvents for the stepwise synthesis, the in situ immobilization of MLs has been successfully achieved, yielding two homometallic mixed-valence copper(I/II) CPs, namely, $[\text{Cu}_4(\text{CN})_3(\text{L1})_2]_n$ (**4**) and $\{[\text{Cu}_4(\text{CN})_3(\text{L3})_2] \cdot 2.5\text{H}_2\text{O}\}_n$ (**6**), as well as an unexpected monovalent copper(I) CP, $[\text{Cu}_2(\text{CN})_2(\text{HL2})]_n$ (**5**), in which the ML units do not exist. All the above-mentioned structures and their synthetic procedures will be discussed in the following text to elaborate the formation of the MLs and the ML-based CPs.

Experimental Section

Materials and Physical Measurements. The chemicals and solvents used in this work were of analytical grade and used as purchased without further purification. Infrared spectra were recorded with a Nicolet Avatar 360 FTIR spectrometer in the range of $4000\text{--}400\text{ cm}^{-1}$ (KBr pellets). Elemental analyses of C, H, and N were determined with a PerkinElmer 2400C elemental analyzer.

Preparations. Ligands HL1–HL3. Refer to previous literature for the syntheses of HL1–HL3.^{8,10} Single crystals of HL2 suitable for X-ray crystallography were grown by solvothermal reaction. HL2 (0.046 g, 0.2 mmol) in 8 mL of acetonitrile was sealed in a 15 mL Teflon-lined stainless steel reactor and then heated in an oven to $140\text{ }^\circ\text{C}$ for 72 h. After the sample was slowly cooled to room temperature at a rate of $6\text{ }^\circ\text{C}\cdot\text{h}^{-1}$, yellow platelet crystals were collected.

$[\text{Cu}(\text{L1})_2]$ (1**).** Refer to previous literature for the synthesis of **1**.^{10a}

$[\text{Cu}(\text{L2})_2]_n$ (2**).** A mixture of Cu_2O (0.015 g, 0.1 mmol), HL2 (0.045 g, 0.2 mmol), and acetonitrile (6 mL) was stirred for 15 min, then transferred and sealed in a 15 mL Teflon-lined stainless steel reactor, which was heated in an oven to $120\text{ }^\circ\text{C}$ for 72 h and then cooled to room temperature at a rate of $6\text{ }^\circ\text{C}\cdot\text{h}^{-1}$. Black cubic crystals of **2** were obtained (52% yield). Anal. Calcd for $\text{C}_{24}\text{H}_{18}\text{CuN}_8\text{O}_2$: C, 56.08; H, 3.53; N, 21.80. Found: C, 56.95; H, 3.57; N, 21.72. IR (KBr, cm^{-1}): 3080 (w), 3019 (w), 1593 (m), 1568 (m), 1491 (s), 1405 (w), 1368 (s), 1327 (m), 1225 (m), 1147 (w), 1061 (m), 1033 (s), 931 (w), 841 (m), 751 (m), 694 (m).

$[\text{Cu}(\text{L3})_2]$ (3a**) and $[\text{Cu}(\text{L3})_2]_n$ (**3b**).** A procedure similar to that utilized for the synthesis of **2** was used, except HL2 was replaced by HL3. Two concomitant crystals, **3a** (brown column) and **3b** (dark green platelet), were found in the same Teflon-lined reactor in ca. 45 and 23% yields, respectively. Anal. Calcd for $\text{C}_{24}\text{H}_{18}\text{CuN}_8\text{O}_2$: C, 56.08; H, 3.53; N, 21.80. Found: C, 56.01; H, 3.59; N, 21.74 for **3a**; C, 56.11; H, 3.48; N, 21.84 for **3b**. IR (KBr, cm^{-1}) for **3a**: 3101 (w), 3031 (w), 1593 (m), 1564 (m), 1487 (s), 1392 (m), 1360 (s), 1311 (m), 1225 (m), 1156 (w), 1061 (w), 1029 (s), 996 (m), 915 (w), 841 (w), 743 (m); for **3b**: 3101 (w), 3027 (w), 1593 (m), 1564 (m), 1486 (s), 1401 (w), 1373 (s), 1319 (w), 1229 (m), 1151 (w), 1061 (w), 1029 (s), 984 (w), 910 (w), 841 (w), 808 (m), 747 (m).

$[\text{Cu}_4(\text{CN})_3(\text{L1})_2]_n$ (4**).** A mixture of CuCN (0.018 g, 0.2 mmol), HL1 (0.023 g, 0.1 mmol), and acetonitrile (8 mL) was stirred for

15 min and then transferred and sealed in a 15 mL Teflon-lined stainless steel reactor, which was heated in an oven to $120\text{ }^\circ\text{C}$ for 72 h and then cooled to room temperature at a rate of $6\text{ }^\circ\text{C}\cdot\text{h}^{-1}$. X-ray quality brown platelet crystals of **4** were obtained in ca. 32% yield. Anal. Calcd for $\text{C}_{27.5}\text{H}_{17.5}\text{Cu}_4\text{N}_{11.5}\text{O}_2$: C, 41.54; H, 2.22; N, 20.26. Found: C, 41.59; H, 2.18; N, 20.21. IR (KBr, cm^{-1}): 3432 (s), 2128 (m), 2087 (m), 1617 (w), 1564 (m), 1486 (m), 1454 (s), 1364 (s), 1339 (w), 1315 (w), 1282 (w), 1213 (w), 1155 (m), 1078 (s), 927 (w), 89 (w), 775 (m), 710 (m).

$[\text{Cu}_2(\text{CN})_2(\text{HL2})]_n$ (5**).** A procedure similar to that utilized in the synthesis of **4** was used, except HL1 was replaced by HL2, and the temperature was adjusted to $130\text{ }^\circ\text{C}$. X-ray quality orange stick crystals and powder products of **5** were obtained in ca. 65% yield. Anal. Calcd for $\text{C}_{14}\text{H}_{10}\text{Cu}_2\text{N}_6\text{O}$: C, 41.48; H, 2.49; N, 20.73. Found: C, 41.52; H, 2.30; N, 20.79. IR (KBr, cm^{-1}): 3227 (m), 3043 (w), 2128 (m), 2103 (s), 1662 (s), 1601 (w), 1580 (w), 1535 (s), 1413 (m), 1364 (w), 1294 (s), 1147 (m), 1057 (m), 955 (w), 841 (w), 751 (m), 694 (m). The reaction gave some dark orange powders and only a few X-ray quality single crystals, but the X-ray powder diffraction (Figure S1 in the Supporting Information) confirmed the purity of the powder products.

$\{[\text{Cu}_4(\text{CN})_3(\text{L3})_2] \cdot 2.5\text{H}_2\text{O}\}_n$ (6**).** Refer to previous literature for the synthesis of **6**.⁸

X-ray Crystallography. Suitable crystals of HL2 and **2–5** were mounted with glue at the end of a glass fiber. Data collection of the crystals was performed with Mo K α radiation ($\lambda = 0.71073\text{ \AA}$) on a Bruker Smart Apex CCD diffractometer at $T = 293(2)\text{ K}$ using SMART.¹¹ Parameters for data collections and refinements of the ligand (HL2) and complexes (**2–5**) are summarized in Table 1. Reflection intensities were integrated using SAINT software,¹² and absorption correction was applied.¹³ The structures were solved by direct methods and on F^2 using the SHELXTL program.¹⁴ Anisotropic thermal parameters were applied to all non-hydrogen atoms. The hydrogen atoms were generated geometrically (C–H = 0.930 \AA). Selected bond lengths and angles for complexes **2–5** are given in Table S1 in the Supporting Information. The bridge C/N atoms of CN^- in the asymmetric units of **4** and **5** are indistinguishable and were assigned randomly as a C or an N atom, but the terminal C/N atoms were refined with a 50% probability of being C- or N-labeled C/N. In complex **4**, the C6 and N6 atoms of L1^- experienced disorder, and they were refined using isotropic temperature factors. Note that twice the formula for deprotonated L1^- ligand is $\text{C}_{24}\text{H}_{18}\text{N}_8\text{O}_2$, but in the formula of $[\text{Cu}_4(\text{CN})_3(\text{L1})_2]_n$, two L1^- ligands comprise $\text{C}_{24.5}\text{H}_{17.5}\text{N}_8.5\text{O}_2$. This situation is caused by the disorder of the C6 and N6 atoms of L1^- in **4**, and, therefore, one set of C6 and N6 and the H attached to C6 are assigned the site occupancy of 0.5.

Results and Discussion

Synthesis of Ligands. The Schiff base ligands were employed for their ease of synthesis and high yield in a single-step reaction from commercial and inexpensive re-

(10) (a) Armstrong, C. M.; Bernhardt, P. V.; Chin, P.; Richardson, D. R. *Eur. J. Inorg. Chem.* **2003**, 1145. (b) Bernhardt, P. V.; Chin, P.; Richardson, D. R. *Dalton Trans.* **2004**, 3342.

(11) SMART, Version 5.060; Bruker Analytical X-ray Systems: Madison, WI, 1997–1999.

(12) SAINT, Version V5.6; Bruker Analytical X-ray Systems: Madison, WI.

(13) Sheldrick, G. M. *SADABS*; University of Göttingen: Göttingen, Germany, 1997 and 2003.

(14) Sheldrick, G. M. *SHELXS-97 and SHELXL-97*; University of Göttingen: Göttingen, Germany, 1997 and 2003.

Table 1. Summary of the Crystal Data and Structure Refinement Parameters for **L2** and **2–5**

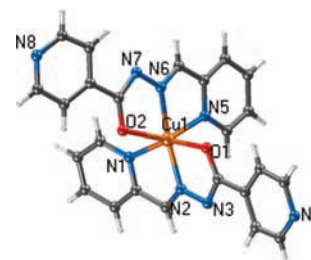
	HL2	2	3a	3b	4	5
formula	C ₁₂ H ₁₀ N ₄ O	C ₂₄ H ₁₈ CuN ₈ O ₂	C ₂₄ H ₁₈ CuN ₈ O ₂	C ₂₄ H ₁₈ CuN ₈ O ₂	C _{27.5} H _{17.5} Cu ₄ N _{11.5} O ₂	C ₁₄ H ₁₀ Cu ₂ N ₆ O
fw	226.24	514.00	514.00	514.00	795.19	405.36
cryst syst	monoclinic	monoclinic	monoclinic	monoclinic	monoclinic	monoclinic
space group	<i>P2(1)/c</i>	<i>P2(1)/c</i>	<i>P2(1)/n</i>	<i>P2(1)/n</i>	<i>P21/a</i>	<i>Pc</i>
<i>a</i> (Å)	12.810(3)	12.3050(11)	7.3626(8)	10.1668(9)	7.9468(6)	6.5040(14)
<i>b</i> (Å)	8.2966(16)	9.7196(9)	14.2319(15)	12.6901(10)	23.0945(16)	9.059(2)
<i>c</i> (Å)	10.503(2)	19.4917(16)	10.2326(11)	17.7561(15)	16.5554(11)	14.156(3)
α (deg)	90	90	90	90	90	90
β (deg)	107.128(4)	105.126(2)	96.747(2)	98.282(2)	100.8890(10)	103.28(0)
γ (deg)	90	90	90	90	90	90
<i>V</i> (Å ³)	1066.8(4)	2250.4(3)	1064.8(2)	2267.0(3)	2983.7(4)	811.8(3)
<i>Z</i>	4	4	2	4	4	2
<i>T</i> (K)	293(2)	293(2)	293(2)	293(2)	293(2)	293(2)
<i>D</i> _{calcd} (g cm ⁻³)	1.409	1.517	1.603	1.506	1.770	1.658
μ (mm ⁻¹)	0.096	1.011	1.069	1.004	2.861	2.631
no. of reflns collected	8857	13694	7276	13877	18346	5098
no. of unique reflns	2469	5158	2553	5176	6743	3070
<i>R</i> (int)	0.0345	0.0226	0.0219	0.0316	0.0446	0.0224
<i>R</i> 1 [<i>I</i> > 2 σ (<i>I</i>)] ^a	0.0596	0.0371	0.0365	0.0852	0.0517	0.0454
w <i>R</i> 2 [<i>I</i> > 2 σ (<i>I</i>)] ^b	0.1464	0.0950	0.0970	0.1751	0.1308	0.0998
<i>R</i> 1 (all reflns) ^a	0.0882	0.0481	0.0418	0.0983	0.0996	0.0575
w <i>R</i> 2 (all reflns) ^b	0.1686	0.1008	0.1006	0.1810	0.1687	0.1060
ρ_{min} (max/min) (e ⁻ Å ⁻³)	0.303/−0.245	0.374/−0.288	0.419/−0.287	0.782/−0.666	0.531/−0.377	0.783/−0.284

^a *R*1 = $\sum |F_o| - |F_c| / \sum |F_o|$. ^b w*R*2 = $[\sum w(F_o^2 - F_c^2)^2 / \sum w(F_o^2)^2]^{1/2}$.

agents.^{8,15} **HL1** is soluble in acetonitrile and methanol, whereas **HL2** and **HL3** are less soluble in common organic solvents, except for DMF, which reduces their reactivity with metal salts by traditional solution methods. Hence, a solvothermal method was used. We used low temperatures (below 120 °C) and short reaction times (72 h) to avoid the hydrolysis of the Schiff bases when coordinating the ligands to the copper ions.

Formation of MLs. As shown in Chart 1, these Schiff base ligands (**HL**) are suitable for forming monomeric units because two ligands provide two sets of imine N and carbonyl O as chelating sites to bind one metal center, forming ML₂ architecture. Therefore, we used a molar ratio of Cu₂O/HL = 1:2 to attain the monomeric ML₂ complexes that contain vacant pendant pyridyl groups for further coordination. Four complexes (**1**, **2**, **3a**, and **3b**) were obtained, and all the ligands in these complexes are deprotonated.⁸ The copper(I) ions are oxidized to copper(II) because the hard base oxygen donors tend to coordinate with copper(II) rather than to copper(I).⁹ However, only **1** and **3a** are discrete complexes and can serve as MLs for constructing extended CPs. The formation of the MLs could also be verified from the IR spectra, in which the N–H (ca. 3440 cm⁻¹) and C=O (ca. 1680 cm⁻¹) stretching of the ligand is missing in the spectra for the complex. A detailed discussion of the IR analysis can be found in our previous communication.⁸

Complex **1** consists of one copper(II) and two deprotonated **L1**⁻ ligands (Figure 1). The ortho-position N atom in the pyridyl ring of **L1**⁻ is responsible for its firmly chelating role, and, thus, the copper(II) center is meridionally bounded by two carbonyl O atoms, two imine N atoms, and two

**Figure 1.** Structure of monomeric complex **1** with labeled atoms.

pyridine N atoms from two **L1**⁻ ligands, completing the distorted octahedral *cis*-N₄O₂ coordination geometry.¹⁰ The dihedral angle between two ligands is 83.8°, and the angle of two pyridine rings with free pyridyl N atoms (N4 and N8) is 110.1°, and, therefore, complex **1** can serve as an angular linker. It is notable that angular linkers with angles around 120° were widely utilized for constructing some impressive coordination architectures, such as polygons, zigzag chains, and helices.¹⁶ The crystal structure of **1** was previously reported by Bernhardt et al.^{10a}

Complex **3a** also consists of one copper(II) and two deprotonated **L3** ligands, but the chelating mode is different from that in complex **1** (Figure 2, view (a)) because the para-position N atom in the pyridyl ring of **L3**⁻ exhibits a bridging mode in the formation of **3a**. The copper(II) center is primarily coordinated with two carbonyl O atoms [Cu–O, 1.9492(15) Å] and two imine N atoms [Cu–N, 2.0108(15) Å], adopting a square-planar *trans*-N₂O₂ geometry [*trans*-O1–Cu1–O1A and *trans*-N1–Cu1–N1A are both 180°].^{4c} The crystal packing of **3a** contains aromatic π – π stacking and intermolecular Cu \cdots N interactions (Figure 2, view (b)). Each copper(II) atom weakly interacts with two N atoms from adjacent molecules in the opposite sides, with the separation of 2.546(2) Å, adopting a pseudo-octahedral

(15) (a) Cozzi, P. G. *Chem. Soc. Rev.* **2004**, *33*, 410. (b) Wezenberg, S. J.; Kleij, A. W. *Angew. Chem., Int. Ed.* **2008**, *47*, 2354. (c) Ganguly, R.; Sreenivasulu, B.; Vittal, J. J. *Coord. Chem. Rev.* **2008**, *252*, 1027. (d) Gupta, K. C.; Sutar, A. K. *Coord. Chem. Rev.* **2008**, *252*, 1420. (e) Zhou, X.-H.; Wu, T.; Li, D. *Inorg. Chim. Acta* **2006**, *359*, 1442.

(16) (a) Abourahma, H.; Moulton, B.; Kravtsov, V.; Zaworotko, M. J. *J. Am. Chem. Soc.* **2002**, *124*, 9990. (b) Huang, X.-C.; Zhang, J.-P.; Chen, X.-M. *J. Am. Chem. Soc.* **2004**, *126*, 13218.

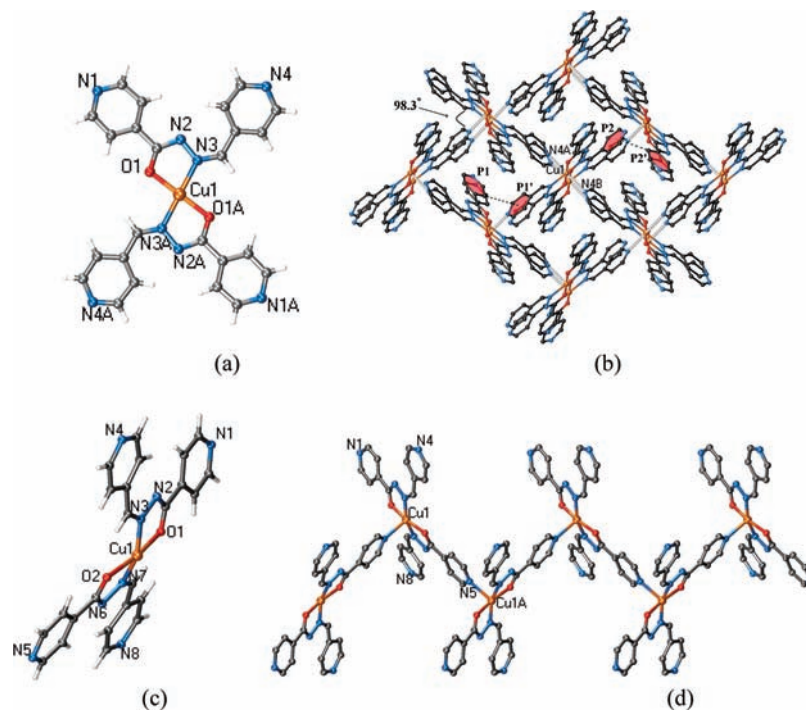


Figure 2. (a) Structure of monomeric complex **3a** with labeled atoms. (b) Perspective view of the stacking array of **3a** showing the formation of a 2D layer through Cu...N intermolecular interactions indicated as gray lines (symmetry code: A: $-x, -y + 1, -z + 1$). (c) Asymmetric unit of complex **3b** with labeled atoms. (d) Perspective view of the 1D zigzag chain structure of **3b** (symmetry code: A: $-x + 3/2, y + 1/2, -z + 1/2$; B: $-x + 3/2, y - 1/2, -z + 1/2$). In (b) and (d), all hydrogen atoms are omitted for clarity.

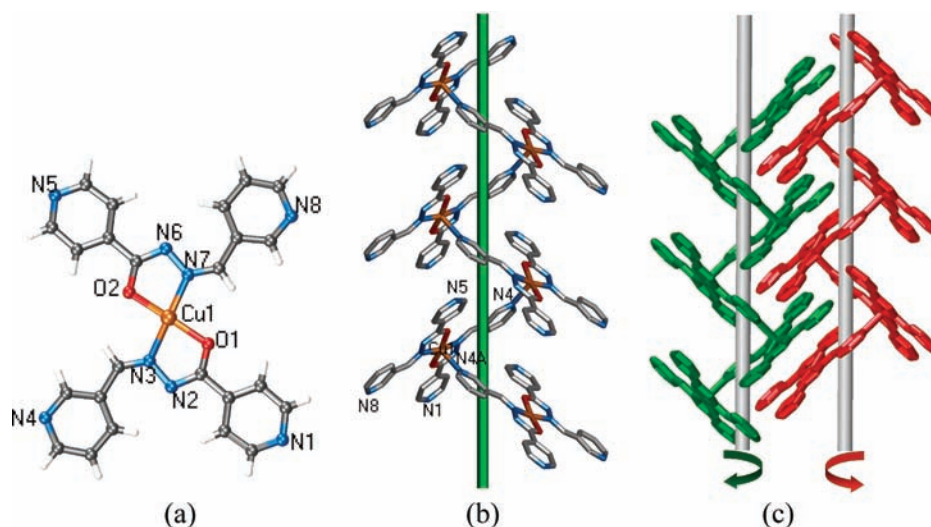


Figure 3. (a) Asymmetric unit of complex **2** with labeled atoms. (b) Perspective view of the 1D helical chain structure of **2** (symmetry code: A: $-x + 1, y + 1/2, -z + 1/2$; B: $-x + 1, y - 1/2, -z + 1/2$). (c) Perspective view of the stacking array of **2** showing the interchain arrangement with alternate helicity (left: green; right: red). In (b) and (c), all hydrogen atoms are omitted for clarity.

coordination geometry. Moreover, each $[\text{Cu}(\text{L}3)_2]$ motif stacks mutually with four neighboring ones through two types of edge-to-face aromatic stacking interactions (between the pyridine rings planes of $P1$ and $P1'$ and $P2$ and $P2'$, shown in Figure 2, view (b)), with the separation of 3.466 Å, and the dihedral angles between two adjacent motifs are 98.3°. To our knowledge, the cases of square-planar MLs with four-coordinated sites are rare, and the bis(Schiff base) ML in this work represents a new family of MLs, which is unique and different from the extensively explored metal–salen Schiff base family.^{4c,15a,b}

Complex **3b** exists concomitantly when generating **3a** in the solvothermal reaction of Cu_2O salts and **HL3** ligand (molar ratio 1:2), and **3a** and **3b** are genuine isomers with the same formula of $[\text{Cu}(\text{L}3)_2]$. In **3b**, each copper(II) atom is five-coordinated by two carbonyl O atoms [Cu–O, 1.920(3)–1.970(3) Å], two imine N atoms [Cu–N, 1.975(4)–1.989(4) Å], and one pyridine N atom [Cu–N, 2.286(4) Å] from three deprotonated $\text{L}3^-$ ligands, adopting a distorted pyramidal environment (Figure 2, view (c)). Different from the situation in **3a**, the two $\text{L}3^-$ ligands in an asymmetric unit of **3b** are not co-planar, with the dihedral angle of 20.1°,

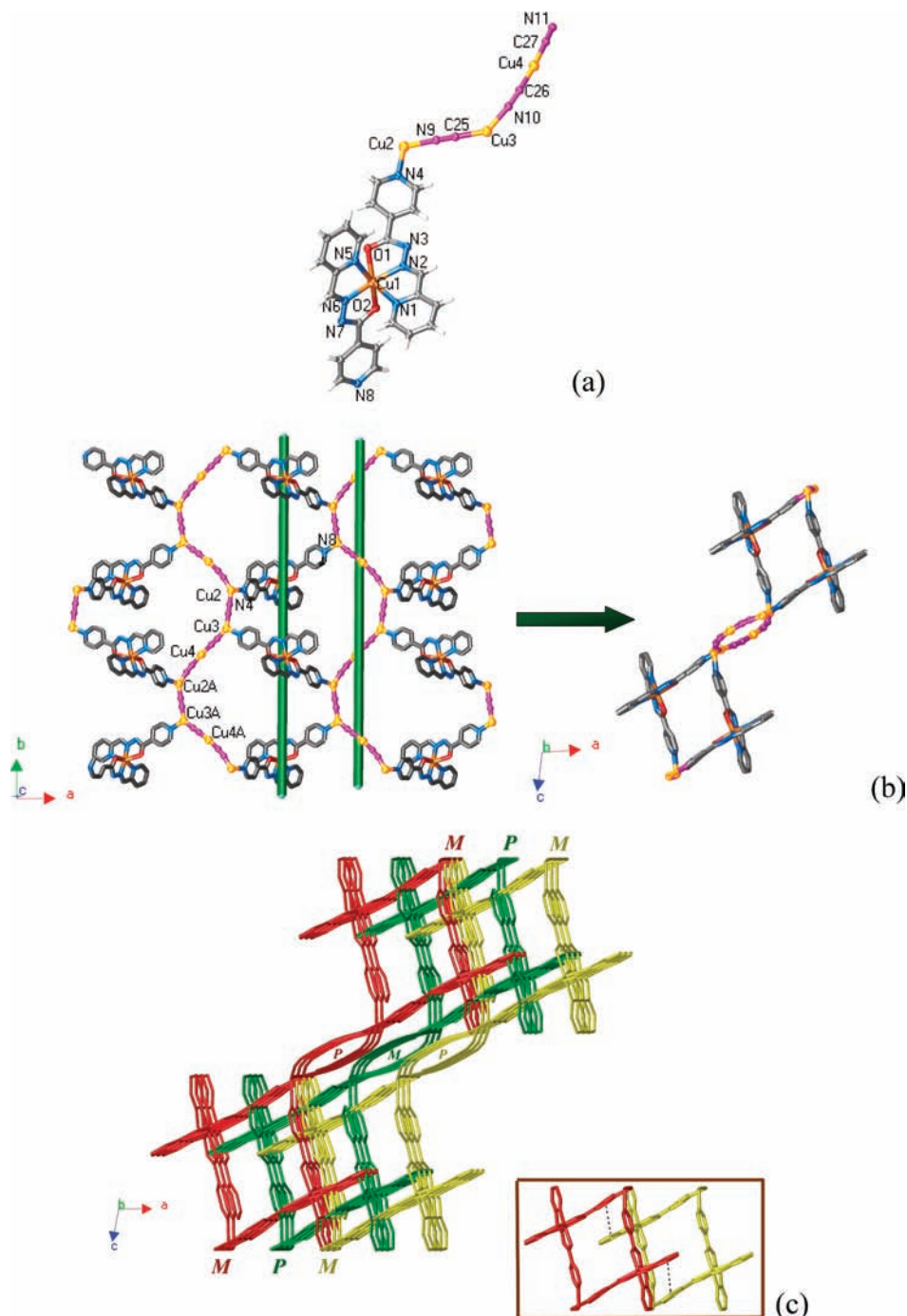


Figure 4. (a) Asymmetric unit of complex **4** with labeled atoms. (b) Perspective view of the 2D tubular layer structure of **4** formed by an alternating assembly of two types of helices, showing side (left) and top (right) views. (c) Perspective view of the stacking array of **4** showing the intercalated adjacent layers with opposite handedness. The inner box shows the interlayer aromatic interactions. In (b) and (c), all hydrogen atoms are omitted for clarity.

and complex **3b** exhibits a 1D zigzag chainlike polymeric structure (Figure 2, view (d)). There also exist offset face-to-face π - π interactions between the pyridyl rings of adjacent chains, with the separation of 3.349 Å. Great efforts were made to obtain the pure products of **3a** and **3b** by varying reaction conditions, such as reagents, solvents, temperature, and time. However, **3a** and **3b** presented as concomitant isomers in all performed conditions with similar yields, implying that the energy gap between the formations of these two isomers is too small to distinguish them from each other.

Exceptional Situation for the Formation of MLs. In an effort to investigate the ligand-geometry effect in this family of copper Schiff base MLs, **HL2** with a meta-position N atom in the pyridyl ring was employed. However, despite varying many reaction conditions, such as copper salts (CuBr, Cu₃N, Cu₂O, CuO, Cu(OH)₂, etc.), solvents and solvent content, reaction time (1–6 days), and temperature (100–140 °C), the reactions of copper salts and **HL2** ligand (molar ratio 1:2) yielded infinite 1D helical chain complex **2**, but not the discrete mononuclear complex [Cu(L2)₂]. In **2**, each copper(II) atom, which adopts a pyramidal *trans*-N₂O₂

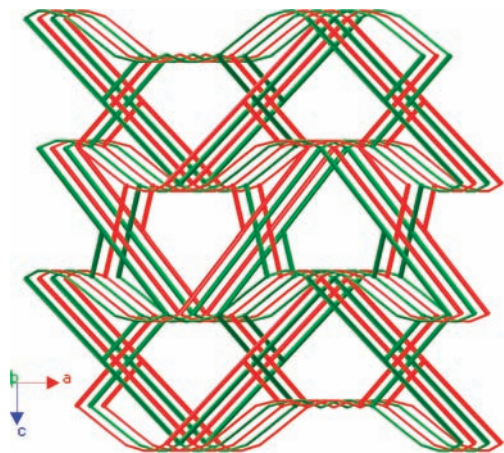


Figure 5. Perspective view of the whole 3D, two-fold interpenetrated network of **6**, showing different interpenetrated identical nets in red and green. The $[\text{Cu}(\text{L}3)_2]$ motifs are simplified to square-planar nodes. All hydrogen atoms and guest water molecules are omitted for clarity.

coordination sphere, is five-coordinated by two carbonyl O atoms $[\text{Cu}-\text{O}, 1.9459(13)-1.9520(13) \text{ \AA}]$, two imine N atoms $[\text{Cu}-\text{N}, 1.9536(15)-1.9628(16) \text{ \AA}]$, and one pyridine N atom $[\text{Cu}-\text{N}, 2.3411(16) \text{ \AA}]$ from three deprotonated $\text{L}2^-$ ligands, with the bond angles around the copper(II) atom in the range of $80.51(6)-172.43(6)^\circ$ (Figure 3, view (a)). Adjacent $[\text{Cu}(\text{L}2)_2]$ motifs, with the dihedral angle of 91.8° , are linked by $\text{Cu}1-\text{N}4\text{A}$ to extend to a 1D helix (Figure 3, view (b)) and 1D helical chains with opposite helicity (left- or right-handedness), alternately stacked with each other through $\pi-\pi$ interactions between parallel pyridyl rings [offset face-to-face distance of 3.460 \AA] to form an achiral 2D packing with the centro-symmetric space group of $P2(1)/c$ (Figure 3, view (c)). It is likely that in the case of $\text{L}2^-$ the failure to synthesize the positional isomers analogous to MLs **1** and **3a** may be due to the distinct coordination abilities of the N position (meta versus para or ortho) in pyridyl rings.¹⁷ The intrinsic diversity of this series of self-assembly processes would be of particular interest to theoretical chemists.

In Situ Immobilization of MLs into CPs. Because of the difference of the *ortho*- and *para*-N-pyridyl substituent, the archetype of **1** differs from that of **3a** with more coordinating sites. Therefore, MLs **1** and **3a** can serve as rigid angular and square-planar “linkers” in the formation of homometallic mixed-valence copper(I/II) CPs, respectively. Due to the poor solubility of **1** and **3a**, which hinders the utilization of stepwise synthesis, we chose simple linear bidentate pseudo-halide CN^- as a bridging spacer to in situ immobilize the MLs into CPs. Solvothermal reactions of CuCN salt and **HL1** or **HL3** (molar ratio 2:1) in similar conditions were performed. As expected, two homometallic mixed-valence copper(I/II) CPs **4** and **6**, which incorporate the ML units of **1** and **3a**, were successfully achieved. Both

4 and **6** contain similar helical $[\text{CuCN}]_n$ chains, whereas the different coordinating geometries of MLs **1** and **3a** led to the structural variation of the resultant CPs **4** and **6**.

Complex **4** exhibits a rare 2D, interdigitated helical tubular layer structure¹⁸ that is composed of alternately arranged fused right-hand (*P*) and left-hand (*M*) helices along the *c* axis. X-ray crystallography shows that **4** crystallizes in the centro-symmetric space group of $P21/a$, with one $[\text{Cu}(\text{L}1)_2]$ and one $[\text{Cu}(\text{CN})_3]$ motif in the asymmetric unit (Figure 4, view (a)). The copper(II) center in the $[\text{Cu}(\text{L}1)_2]$ unit adopts a distorted octahedral coordinating geometry, similar to that in **1**. There are three crystallographically independent copper(I) ions in the $[\text{CuCN}]_n$ chains. Cu(2) and Cu(3) are both three-coordinated by one pyridine N atom $[\text{Cu}(2)-\text{N}(4), 2.073(4) \text{ \AA}; \text{Cu}(3)-\text{N}(8), 2.086(4) \text{ \AA}]$ and two C/N atoms from cyanide groups $[\text{Cu}(2)-\text{C/N}, 1.901 \text{ \AA}; \text{Cu}(3)-\text{C/N}, 1.873 \text{ \AA}]$ in a T-shaped geometry, whereas Cu(4) is only bound by two C atoms from two cyanide groups, adopting a linear mode with the bond angle of $174.0(3)^\circ$ (Figure 4, views (a) and (b)). The angular $[\text{Cu}(\text{L}1)_2]$ linker, with the angle of 110.1° , which is also observed in ML **1**, plays a significant role in the formation of the helical tubular layer structure of **4** (Figure 4, view (b)). The neutral angular corners are bridged by $[\text{Cu}-\text{CN}]$ spacers to form an infinite helical chain that is extended along the 2_1 screw axis with a pitch of 23.1 \AA and a tubular channel of about $9.3 \times 9.0 \text{ \AA}$. Another type of helical fragment in the layer is an infinite helical $[\text{CuCN}]_n$ chain along the 2_1 screw axis, with the same pitch, but with opposite handedness compared to the former helix. Furthermore, adjacent layers pack tightly with each other through the intercalation of adjacent helical chains formed by the $[\text{Cu}(\text{L}1)_2]$ motifs (offset face-to-face distance between pyridine rings of 3.515 and 3.522 \AA , intercalation extent 4.65 \AA), displaying a unique alternately arranged helicity fashion (Figure 4, view (c)).

Complex **6** is more complicated, with an unprecedented entangled character,^{19–21} due to the immobilization of the square-planar $[\text{Cu}(\text{L}3)_2]$ motifs, as identified in ML **3a**. The four-coordinated square-planar copper(II) ions are all coordinated in the $[\text{Cu}(\text{L}3)_2]$ motifs, exhibiting the typical character of unsaturated metal centers (UMCs).^{1c,4c} The tetrahedral or trigonal-planar copper(I) ions all lie in the infinite pseudo-helical $[\text{CuCN}]_n$ chains along *a* direction, which are linked by $[\text{Cu}(\text{L}3)_2]$ MLs to form the homometallic mixed-valence copper(I/II) CP. As a whole, complex **6** (if the half-occupied Cu(2) site is considered as always present) is a 3D, two-fold interpenetrated network (Figure 5) related by simply translation (Class Ia)^{20c} with a complex trinodal

(17) (a) Wang, Y.-T.; Tong, M.-L.; Fan, H.-H.; Wang, H.-Z.; Chen, X.-M. *Dalton Trans.* **2005**, 424. (b) Lu, X.-Q.; Jiang, J.-J.; Loye, H.-C.; Kang, B.-S.; Su, C.-Y. *Inorg. Chem.* **2005**, *44*, 1810. (c) Fezell, R. P.; Carson, C. E.; Klausmeyer, K. K. *Inorg. Chem.* **2006**, *45*, 935.

(18) Han, L.; Hong, M.; Wang, R.; Luo, J.; Lin, Z.; Yuan, D. *Chem. Commun.* **2003**, 2580.

(19) (a) Batten, S. R.; Robson, R. *Angew. Chem., Int. Ed.* **1998**, *37*, 1460. (b) Batten, S. R. *CrystEngComm.* **2001**, *3*, 67.

(20) (a) Carlucci, L.; Ciani, G.; Proserpio, D. M. In *Making Crystals by Design. Methods, Techniques and Applications*; Braga, D. F., Grepioni, F., Eds.; Wiley & Sons: New York, 2007; Chapter 1.3, pp 58–85. (b) Carlucci, L.; Ciani, G.; Proserpio, D. M. *Coord. Chem. Rev.* **2003**, *246*, 247. (c) Blatov, V. A.; Carlucci, L.; Ciani, G.; Proserpio, D. M. *CrystEngComm.* **2004**, *6*, 378.

(21) (a) Zhan, S.-Z.; Li, D.; Zhou, X.-P.; Zhou, X.-H. *Inorg. Chem.* **2006**, *45*, 9163. (b) Zhou, X.-P.; Ni, W.-X.; Zhan, S.-Z.; Ni, J.; Li, D.; Yin, Y.-G. *Inorg. Chem.* **2007**, *46*, 2345.

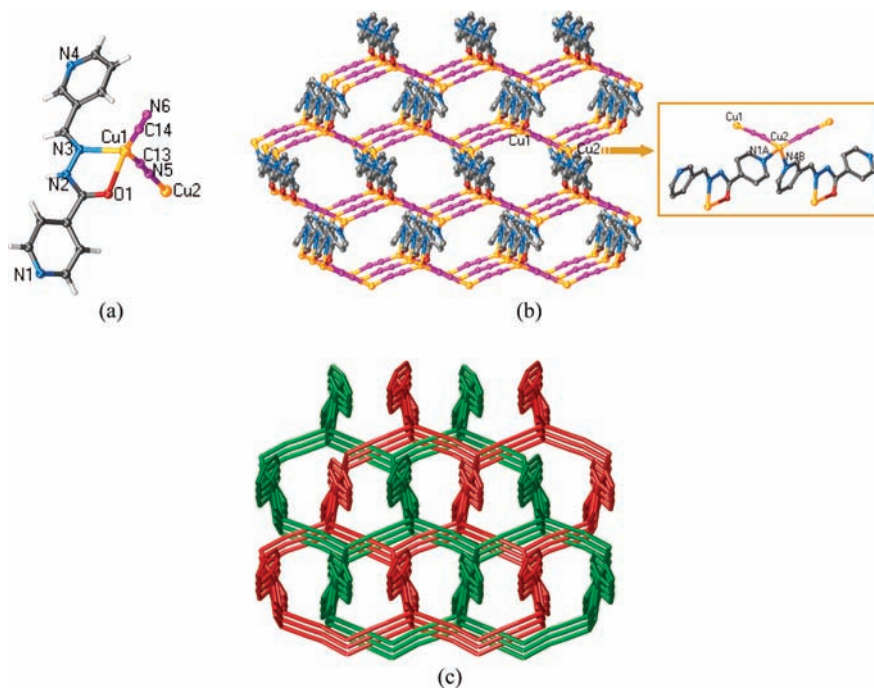


Figure 6. (a) Asymmetric unit of complex **5** with labeled atoms. (b) Perspective view of the 3D diamondoid structure of **5** (symmetry code. A: $x, y - 1, z$; B: $x - 1, -y + 1, z + 1/2$; C: $x - 1, -y + 1, z - 1/2$; D: $x + 1, -y + 1, z - 1/2$; E: $x + 1, -y + 1, z + 1/2$; F: $x, y + 1, z$). The inner box shows the constructing unit (NOT an ML) in the framework of **5**. (c) Perspective view of the 3D, two-fold interpenetrated network of **5**, showing different interpenetrated identical nets in red and green. In (b) and (c), all hydrogen atoms are omitted for clarity.

(3,4)-connected net with nodes so defined: $(3\text{-c Cu}_3)_2(4\text{-c Cu}_1)(4\text{-c Cu}_2)$ with point symbol $\{8^3\}_2\{8^5\cdot 10\}\{8^6\}$ (see page S5 in the Supporting Information for a detailed topological analysis).

Exceptive Situation for the In Situ Immobilization of MLs. Although the isolation of a discrete monometallic ML based on $\mathbf{L}2^-$ was not achieved, as mentioned in the above text, the $[\text{Cu}(\mathbf{L}2)_2]$ motif was incorporated in the resulting CP **2**. This prompted us to attempt in situ immobilization of the $[\text{Cu}(\mathbf{L}2)_2]$ ML into CP. Unexpectedly, the structure of **5**, yielded by the similar reaction conditions for generating **4** and **6**, does not contain the $[\text{Cu}(\mathbf{L}2)_2]$ motif observed in **2**. Complex **5** is a 3D, two-fold interpenetrated diamondoid network, in which **HL2** ligands are not deprotonated and, thus, do not chelate copper(II) ion to form a four-coordinated square-planar ML, like that in **6**. The neutral form of **HL2** can also be verified by IR spectroscopic data, where the absorption band at 3227 cm^{-1} occurred because of the amide N–H stretching vibration. In this regard, we assume the lack of oxidation of the copper(I) to copper(II) may be related to the deprotonation of the Schiff base ligand and the formation of the MLs. The asymmetric unit of **5** consists of two monovalent copper atoms, two cyanide groups, and one neutral **HL2** ligand (Figure 6, view (a)). The Cu(1) atom adopts a distorted tetrahedral geometry and is occupied by one carbonyl O atom [Cu–O, 2.223(4) Å], one imine N atom [Cu–N, 2.160(4) Å], and two C/N atoms [Cu–C/N, 1.864(5)–1.857(5) Å] from two bridging cyanide groups. Cu(2) also has a distorted tetrahedral environment that is coordinated by two pyridyl N atoms [Cu–N, 2.094(5)–2.138(5) Å] and two cyanide C/N atoms [Cu–C/N, 1.963(9)–2.003(6) Å]. The copper(I) ions are bridged by cyanide anions to form infinite zigzag chains, and the $[\text{CuCN}]_n$ chains are further

linked by **HL2** ligands, arranging in an ABAB repeating fashion to extend to a 3D diamondoid network (Figure 5 view (b)). Furthermore, two identical diamondoid nets interpenetrate with each other in a common parallel fashion (Figure 5, view (c)). The unexpected situation in the structure of **5**, compared to those of **4** and **6**, reminds us to take into consideration the symmetry factor in forming MLs and their in situ immobilization into CPs. As suggested in recent literature, the degree of structural manipulation may be dramatically affected by the symmetry of the bridging ligands or metal binding sites, and, thus, symmetry considerations for designing “connectors and linkers” are important.^{6a,22} In contrast to $[\text{Cu}(\mathbf{L}1)_2]$ (**1**) and $[\text{Cu}(\mathbf{L}3)_2]$ (**3a**) MLs, the $[\text{Cu}(\mathbf{L}2)_2]$ motif is obviously less symmetrical because it contains both *meta*- and *para*-pyridyl N groups as potential bridging sites (Figure 3, view (a)). Therefore, the self-assembly process of CuCN and **HL2** favors constructing the highly symmetrical 3D diamondoid network **5**, discarding the trend for the in situ immobilization of the $[\text{Cu}(\mathbf{L}2)_2]$ ML.

Conclusion

In this work, we have taken advantage of a proposed synthetic algorithm, namely, the in situ immobilization of metalloligands (MLs), to achieve homometallic mixed-valence copper(I/II) Schiff base coordination polymers (CPs). In expatiation, we have designed and synthesized three structurally isomeric Schiff base ligands, bearing both chelating and bridging coordination sites for targeting designer MLs. The solvothermal reactions of corresponding

(22) (a) Halper, S. R.; Malachowski, M. R.; Delaney, H. M.; Cohen, S. M. *Inorg. Chem.* **2004**, *43*, 1242. (b) Kobayashi, Y.; Kawano, M.; Fujita, M. *Chem. Commun.* **2006**, 4377.

copper salts and Schiff base ligands have been properly performed by varying anions and reagent ratios, which produces a new family of metal–bis(Schiff base) MLs and implements the in situ immobilization of these MLs into homometallic mixed-valence copper(I/II) CPs. Moreover, two unexpected compounds based on *meta-N*-pyridyl ligands have been obtained and compared with the para- and ortho-positional analogues, indicating the symmetry of the MLs should be properly considered in developing this synthetic algorithm. We believe this work would provide an insightful synthetic route to prepare useful homometallic mixed-valence CPs.

Acknowledgment. This work was financially supported by the National Natural Science Foundation of China (Grant Nos. 20571050 and 20771072) and the National Science Foundation for Distinguished Young Scholars of China (Grant No. 20825102).

Supporting Information Available: Crystal data and additional structural data and analyses. This material is available free of charge via the Internet at <http://pubs.acs.org>.

IC8015244